17th Symposium IMEKO TC4, 3rd Symposium IMEKO TC19 and 15th IWADC Workshop
Instrumentation for the ICT Era
Sept. 8-10, 2010, Kosice, Slovakia

Pipelined Analog-Digital Converters Integral Nonlinearity Modeling for Post-Correction

Samer Medawar[1], Peter Händel[1], Niclas Björsell[2], Magnus Jansson[1]

[1]*Signal Processing Lab, ACCESS Linnaeus Center, Royal Institute of Technology, SE-100 44 Stockholm, Sweden*
[2]*Department of Electronics, University of Gävle, SE-801 76 Gävle, Sweden*

Abstract- An input-dependent integral nonlinearity (INL) model is developed for pipeline ADC post-correction. The INL model consists of a static and dynamic part. The INL model is subtracted from the ADC digital output for compensation. Static compensation is performed by adjacent sets of gains and offsets. Each set compensates a certain output code range. The frequency content of the INL dynamic component is used to design a set of filter blocks that performs ADC compensation in the time domain. The compensation scheme is applied to measured data of two 12-bit ADCs of the same type (Analog Devices AD9430). Significant performance improvements in terms of spurious free dynamic range (SFDR) are obtained.

I. Introduction

Error correction is a crucial task in a wireless digital communication system. Correction schemes span all the layers in the open system interconnection (OSI) model. In this work, a compensation scheme is developed on the analog-digital converter (ADC) level, which is a pervasive device in any digital telecommunication system. The pipeline structure is typical for ADCs working at the intermediate frequency (IF) of a radio frequency (RF) system. Its structure consists of several subranging stages leading up to a final flash ADC. Each stage resolves a fraction of the ADC output code k, prior to arriving at the final residual that is resolved by the flash ADC.

The ADC can be compensated by tuning some of its inner blocks, however, this approach imposes constraints on the hardware. Another alternative is post-correction, where correction values are added to the ADC digital output depending on the characteristics of the latter. Such post-correction can be made by the means of look-up-tables (LUTs) [1]–[6]. LUTs can be static and dynamic. Static LUT consists of a compensation block that adds a correction term ε_k for every ADC output code k. However, due to the ADC performance dependence on input signal characteristics such as slope or frequency, dynamic LUTs are developed. In this fashion, the LUT is a multidimensional table having the code k as one entry and the ADC input characteristic(s) such as the frequency, slope or previous sample(s), as the other entry(entries). LUT achieves significant ADC performance improvements, however, they are memory consuming, especially dynamic (multidimensional) LUTs.

In this work, a model-based ADC post-correction is investigated based on dynamic integral nonlinearity (INL) models. ADCs INL is a well studied topic in the literature. Static (i.e. only output code k dependency) INL modeling was investigated in [7]–[11]. A dynamic one term INL model having the slope as the dynamic entity was presented in [12]. In [13]–[16], the INL was modeled by a combination of a static high code frequency (HCF) and a dynamic low code frequency (LCF) term, where the input frequency m was the dynamic entity. The HCF was modeled by piecewise linear segments centered around zero, and the LCF by polynomials with frequency dependent coefficients. Such a dynamic model is of interest since it can be translated into a model-based post-correction scheme, who's main advantage over a LUT is that it requires less parameter storage.

II. Dynamic INL Modeling

The end-point quantization is adopted for the simplicity of the post-correction concept presentation in the following paragraph. For a given ADC, with ideal T_k and practical $T[k]$ code transition levels (in [Volt]) as illustrated in Fig. 1, the INL is written as [17]

$$i[k] = \frac{T_k - G\,T[k] - V_{\text{os}}}{Q} \qquad \text{[LSB]} \tag{1}$$

Email: samer.medawar@ee.kth.se

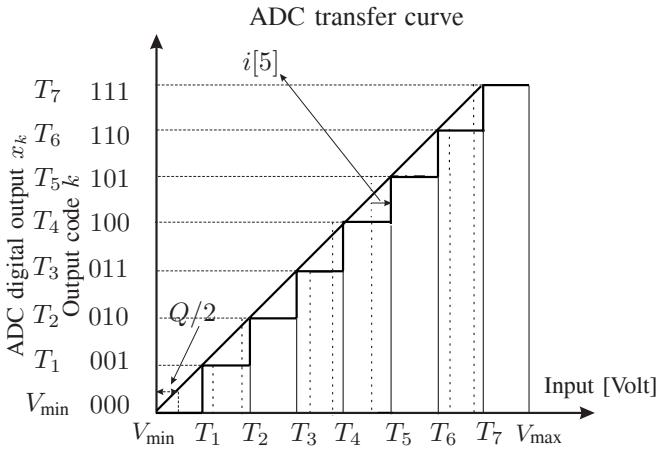

Fig. 1. Ideal (solid line) and practical (dashed line) 3-bit mid-riser ADC transfer curve. The practical ADC is compensated for gain and offset errors. The ideal transition levels T_k coincide with the solid vertical bars while the practical transition levels $T[k]$ (not shown for simplicity) coincide with the dashed bars [15].

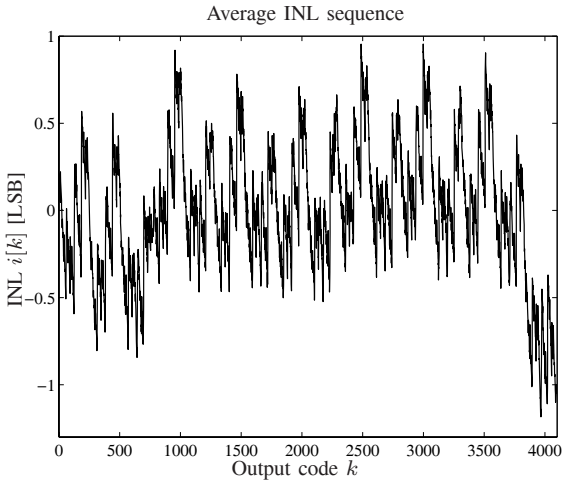

Fig. 2. The plot shows the average INL for 15 sequences corresponding to test frequencies in the interval 30-90 MHz for a 12-bit pipelined ADC (AD9430) [15].

where G and V_{os} are gain and offset terms that can be computed by different procedures as given in [17]. Q is the ideal code bin width or $(V_{\text{max}} - V_{\text{min}})/(2^N)$; N is the number of bits of the ADC. A typical averaged INL sequence of a 12-bit pipelined ADC (AD9430) is shown in Fig. 2. However, the INL has shown a dependence on the input frequency m, and will be further denoted as $i[m, k]$. In [15], the measured INL was described by a parametric model $i_{m,k}$ where m corresponds to the test frequency (that is, f_m in Hz) and k to the ADC output code:

$$i_{m,k} = h_k + \ell_{m,k}\,. \tag{2}$$

where h_k is the HCF component, and $\ell_{m,k}$ is the dynamic LCF component. The HCF component h_k is modeled by a set of P disjoint segments centered around zero that depend on the output code k. The LCF is modeled by a smooth polynomial of order L, with frequency dependent coefficients, over the code k range. Thus, the INL model is further detailed to [15]

$$i_{m,k} = \underbrace{\eta_p\, k + \beta_p}_{h_k} + \underbrace{\theta_{0,m} + \bar{k}\,\theta_{1,m} + \ldots + \bar{k}^l\,\theta_{l,m} + \ldots + \bar{k}^L\,\theta_{L,m}}_{\ell_{m,k}} \tag{3}$$

for an output code k belonging to the segment p, where $p = 1, \ldots, P$. η_p is the slope of the segment p and β_p is an offset. m represents the measured frequency $\{f_m\}_{m=1}^{M}$ where $\bar{k} = (k - 2^{N-1})/(2^{N-1} - 1)$ is a normalized ADC output code.

III. INL-based Post-Correction

The compensation method is derived from the dynamic INL model presented in the previous section. The post-correction scheme is composed of two components: a static remapping of the ADC output and a filter structure composed of linear time-invariant filters.

The endpoint representation for the ADC output is used in this section (refer to Fig. 1), but similar concept applies to the mid-point case. First, a static INL is used for illustrating the post-correction concept, and then the method is extended after to the dynamic INL model.

The transition levels of an ideal and practical ADC (compensated for gain and offset) are illustrated in Fig. 1. Despite having transition levels that deviate from the ideal ones, the digital output of a practical ADC

is indistinguishable from its corresponding ideal ADC output. For an end-point quantization (Fig. 1), the ADC digital output x_k equates to the transition levels, T_k or

$$x_k = T_k \; = T[k] + Q\, i[k]\,. \tag{4}$$

where the second equality comes from (1) for a gain and offset compensated ADC. Having an end-point presentation, a practical ADC yields T_k, corresponding to the transition level $T[k]$. For an endpoint correction, the ADC output x_k is remapped to the corrected output $\widehat{s}_k = x_k + \varepsilon_k$, where ε_k is determined from

$$\widehat{s}_k = T[k] = x_k - Q\, i[k] \tag{5}$$

to be $\varepsilon_k = -Q\, i[k]$. The integer m, corresponding to frequency f_m Hz, differentiates the different input stimuli. Thus, the static INL term $i[k]$ is in turn replaced by the M-dimensional $i[m,k]$, where $m = 1, \ldots, M$. In the post-correction block-model, the LUT $i[m,k]$ is replaced by a parametric model $\widehat{i}_{m,k}$, where "$\widehat{\ }$" means least-squares estimated model based on $i_{m,k}$ in (2); in other words, the correction term is

$$\varepsilon_{k,m} = -Q\,\widehat{h}_k - Q\,\widehat{\ell}_{m,k}\,. \tag{6}$$

A. HCF Post-Correction

The P centered HCF segments represent the abrupt changes in the INL and are used for a direct remapping of the ADC output. The static compensation term $\widehat{h}_k$ is derived from the HCF model in (6) and is given by

$$\widehat{h}_k = \widehat{\eta}_p\, k + \beta_p \qquad k_{p-1} \le k < k_p \tag{7}$$

where β_p is a known offset, $\beta_p = -\widehat{\eta}_p(k_p + k_{p-1} - 1)/2$, and k_p are the segments borders $p = 1, \ldots, P$ [15].

B. LCF Post-Correction

The LCF model is constructed out of a set of frequency dependent polynomials. Each polynomial represents a measured LCF data for a certain frequency f_m in the bandwidth under test. Thus, considering the ADC normalized code $\bar{k}$ and its powers $\bar{k}^l$ of the LCF polynomials, one can note that they are weighted by a frequency-dependent factor $\theta_{l,m}$. In other words, the output code power $\bar{k}^l$ contributes to every LCF model polynomial by the factor $\theta_{l,m}$. Thus, for a given output code $\bar{k}$, the entity $\theta_{l,m}$ can be considered as sample points of a given filter frequency function $G_l(\nu)$ with input $\bar{k}^l$. Having real-valued polynomial coefficient $\theta_{l,m}$, the frequency function $G_l(\nu)$ is written as

$$G_l(\nu_m) = \theta_{l,m} \qquad \text{where} \qquad \nu_m = 2\pi f_m / f_s \tag{8}$$

where f_s is the sampling frequency. The ADC post-correction is performed in the time domain by linear filtering of the ADC normalized output $\bar{k}$ followed by a multiplication of the output with $\bar{k}^{l-1}$. Thus, the time response of the filters $G_l(\nu)$ is to be derived from their respective frequency responses given by (8). The inverse fast Fourier transform is an adequate method [18]–[20] to calculate the filter coefficients in the time domain from the considered sampled frequency response. The concept lies in designing a proper IFFT filter based on a specification in the frequency domain. However, the design details are out of the scope of this paper. [18]–[20] present different approaches on this topic. Denoting the resulting impulse response by $g_l[n]$ for $l = 1, \ldots, L$, the dynamic post-correction term $-Q\,\widehat{l}_{m,k}$ in (6) is given by

$$-Q\,\left(\sum_{l=1}^{L}\left(\left(g_l[n] * \bar{k}[n]\right)\;\bar{k}^{l-1}[n]\right) + \theta_0\right) \tag{9}$$

where $*$ denotes convolution, θ_0 is the average of $\{\theta_{0,m}\}_{m=1}^{M}$, and $\bar{k}[n]$ has been indexed by n to indicate its time dependence.

The filters coefficients are computed once and used during the whole post-correction process. Since two ADCs are in disposition, two different post-correction blocks are obtained. The structure of the post-correction block is shown in Fig. 3.

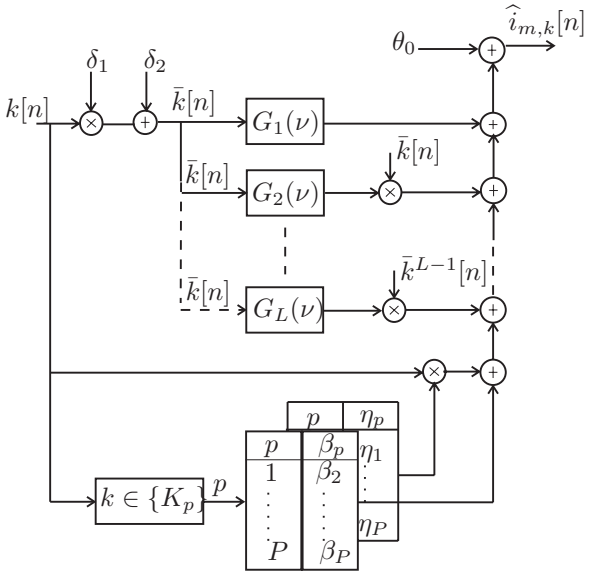

Fig. 3. ADC post-correction block with ADC code $k[n]$, as input. δ_1 and δ_2 are defined as $\delta_1 = 1/(2^{N-1}-1)$ and $\delta_2 = -2^{N-1}/(2^{N-1}-1)$. The ADC output code k is indexed by n to indicate its time dependence. The output is the correction term $\widehat{i}_{m,k}[n]$ [16].

IV. Test set-up and device under test

The INL has been characterized for the 30-90 MHz band, using two samples of the Analog Devices AD9430. The ADC output sequences are collected for specific input frequencies spanning the bandwidth with a frequency step of 5 MHz. The frequencies are fine-tuned to fulfill the coherent sampling conditions [17]. The two ADC samples will be denoted in the sequel as ADC1 and ADC2. The employed ADC test setup for INL testing is described in [15]. The INL and the post-corrected data measurements were done simultaneously. For the INL measurements case, the ADC input is slightly overdriven according to [17], while the post-corrected data is measured at a -0.5 dBFS according to the AD9430 datasheet. Information about the test bed in general can be found in [21]. In wideband systems, the SFDR, SINAD, noise and IMD of an ADC are the crucial parameters [17].

V. Results

Single tone signals, spanning the bandwidth of use, were input to the ADC, where the post-correction method was applied on the acquired output. As an illustration, the SFDR improvement for a 60-MHz signal sequence is shown in Fig. 4. A 12.5-dB SFDR improvement is obtained, whereas all harmonics are rescinded and the spurious are reduced to near the noise level.

Fig. 5 summarizes the improvements in terms of SFDR for ADC1 and ADC2. Three methods are used to compensate the ADCs. The developed INL-based post-correction model, a static LUT compensation based on averaged INL data and the INL sequence for every input frequency (self-calibration or dynamic LUT). Both ADCs undergo significant improvement in terms of SFDR over the band of use. The model compensation method, however, when compared to the LUT methods, differs for the two ADCs. Considering ADC1, the INL model can perform an almost identical correction to the dynamic LUT. The model outperforms the self-calibration for some singular frequencies by the order of 0.5 to 1 dB. Self-calibration is superior by 1 dB at the 90 MHz frequency. One can explain this by the fact that the INL at these high frequencies is quite noisy; thus, the model cannot grasp much of the INL information, as shown in [15]. Model compensation is almost uniformly superior than the static LUT compensation although it consists of significantly less number of parameters. ADC2 did not encounter improvements in the order of 13.3 dB, but it has more stable improvements over the entire bandwidth. However, the difference between the LUT and the model is higher when compared to ADC1. Referring also to [15], the model was not able to mimic the data as well as for ADC1, which is due to the noisier INL of ADC2 over the whole bandwidth (compared

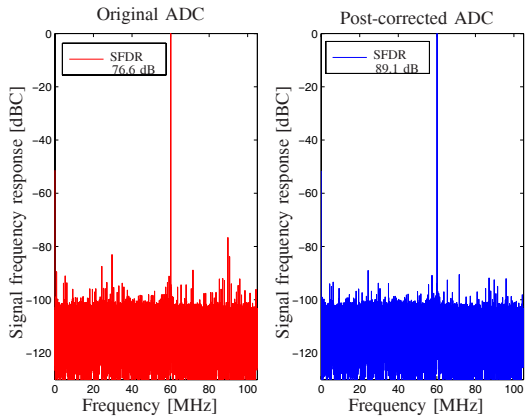

Fig. 4. SFDR improvement of a 60-MHz signal sequence.

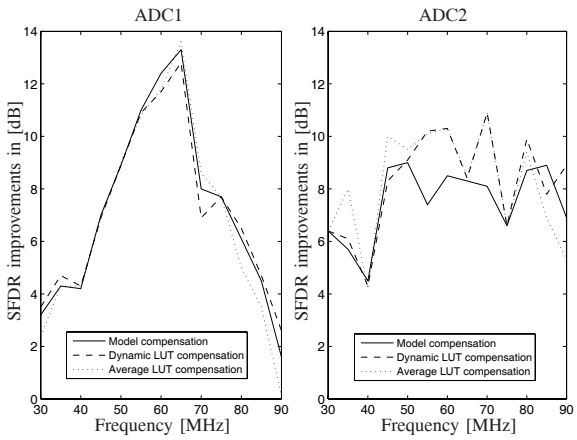

Fig. 5. SFDR improvement for ADC1 and ADC2 over the band of use [16].

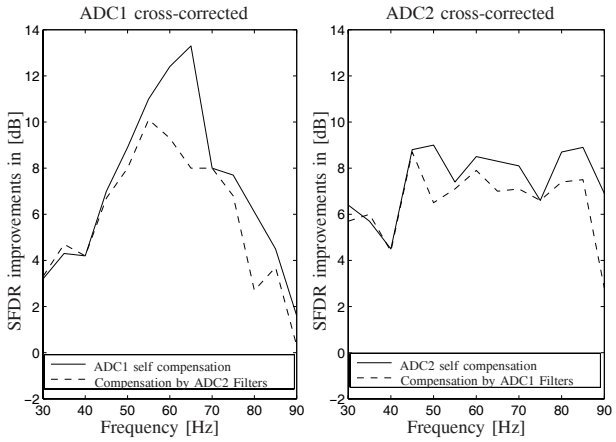

Fig. 6. ADC1 and ADC2 cross-compensation.

to ADC1). Moreover, the static part of ADC2 INL is more pronounced than ADC1 while the model comprises mostly dynamic parameters. More results (including SINAD, IMD and Noise improvements) and explanations are presented in [16].

In order to test the reliability and robustness of the post-correction schemes developed, a cross compensation is performed. In other words, ADC1 post-correction model is used to compensate ADC2, and vice-versa. Being based on the HCF segments, the static post-correction block is tailored for each ADC, thus it is omitted in this cross compensation. Only the filter banks (of ADC1 and ADC2) are used, since their respective LCF models (of ADC1 and ADC2) are similar in structure and magnitude. The results of the cross-compensation are shown in Fig. 6. The two cross-compensated ADCs encounter SFDR performance improvements quite similar to the self-compensation (filter banks and segments) over the entire bandwidth. The high improvements encountered by ADC1 in the middle band are a bit smothered by the cross-compensation. The same applies for the high frequencies of ADC2. However, cross-compensation can occasionally outperform the self-correction for some input frequencies. Thus, the frequency content of the LCF model can be used for cross-ADC correction or for developing a general post-correction scheme.

VI. Conclusions

ADC model-based post-correction based on the INL-model showed to be a reliable method while presenting low complexity. The developed INL-model-based post-correction method was shown to perform quite similarly to a

LUT approach. INL modeling in terms of the frequency (in addition to the ADC output code k) proved to be a highly versatile tool because the implicit frequency information can be used for developing a rather simple filter model for post-correction. The filters demonstrated their capability to reconstruct the INL information. Such a filter approach is in favor of a LUT in the sense that it requires the storage of significantly fewer parameters and needs no interpolations or approximations to compensate input frequencies that differ from calibration frequencies. More detailed results can be found in [16].

References

[1] T. A. Rebold and F. H. Irons, "A phase-plane approach to the compensation of high-speed analog-to-digital converters," in *Proc. IEEE Int. Symp. Circuits Syst.,* vol. 2, 1987, pp. 455-458.

[2] F. H. Irons, D. M. Hummels, and S. P. Kennedy, "Improved compensation for analog-to-digital converters," *IEEE Trans. Circuits Syst.,* vol. 38, no. 8, pp. 958-961, Aug. 1991.

[3] D. M. Hummels, F. H. Irons, and S. P. Kennedy, "Using adjacent sampling for error correcting analog-to-digital converter", in *Proc. IEEE Int. Symp. Circuits Syst.,* vol. 2, 1992, pp. 589-592.

[4] P. Händel, M. Skoglund, and M. Pettersson, "A calibration scheme for imperfect quantizers," *IEEE Trans. Instrum. Meas.* 49 (2000), pp. 1063-1068

[5] H. Lundin, M. Skoglund, and P. Händel, "A criterion for optimizing bit-reduced post-correction of AD converters," *IEEE Trans. Instrum. Meas.,* vol. 43, no. 4, pp. 1159-1166, Aug. 2004.

[6] H. Lundin, M. Skoglund, and P. Händel, "Optimal index-bit allocation for dynamic post-correction of analog-to-digital converters," *IEEE Trans. Signal Process.,* vol. 53, no. 2, pp. 660-671, Feb. 2005.

[7] L. Michaeli, P. Michalko and J. Saliga, "Identification of ADC error model by testing of the chosen code bins," *12:th IMEKO TC4 International Symposium*, September 25-27, 2002, Zagreb, Croatia.

[8] L. Michaeli, P. Michalko, and J. Saliga, "Identification of unified ADC error model by triangular testing signal," *10th Workshop on ADC modelling and testing*, Gdynia/Jurata, Poland, pp. 605-610, 2005.

[9] A. Cruz Serra, F. Alegria, L. Michaeli, P. Michalko, J. Saliga, "Fast ADC testing by repetitive histogram analysis," *IEEE Instrumentation and Measurement Technology Conference*, April 24-27, 2006, pp. 1633-1638.

[10] L. Michaeli, P. Michalko, J. Saliga, "Unified ADC nonlinearity error model for SAR ADC," *Measurement* Vol. 41, Issue 2, pp. 198-204, February 2008.

[11] A.C. Serra, M.F. da Silva, P.M. Ramos, R.C. Martins, L. Michaeli and J. Saliga, " Combined spectral and histogram analysis for fast ADC testing," *IEEE Transactions on Instrumentation and Measurement*, Vol. 54, No. 4, pp. 1617-1623, August 2005.

[12] P. Arpaia, P. Daponte and L. Michaeli, "A dynamic error model for integrating analog-to-digital converters," *Measurement* 25, pp. 255-264, June 1999.

[13] N. Björsell and P. Händel, "Dynamic behavior models of analog to digital converters aimed for post-correction in wideband applications," *11th Workshop on ADC Modelling and Testing*, September 17-22, 2006, Rio de Janerio, Brazil.

[14] P. Händel, N. Björsell and M. Jansson, "Model based dynamic characterization of analog-digital-converters at radio frequency— Invited paper," *2007 International Conference on Signal Processing and its Applications*, 12-15 February 2007, Sharjah, UAE.

[15] S. Medawar, P. Händel, N. Björsell and M. Jansson, "Input dependent integral nonlinearity modeling for pipelined analog-digital converters," *IEEE Transactions on Instrumentation and Measurements*, in press, December 2009, doi: 10.1109/TIM.2010.2045551.

[16] S. Medawar, P. Händel, N. Björsell and M. Jansson "Postcorrection of pipelined analog-digital converters based on input dependent integral nonlinearity modeling," *IEEE Transactions on Instrumentation and Measurement*, *accepted for publication*, May 2010.

[17] *IEEE Standard for Terminology and Test Methods for Analog-to-Digital Converters*, IEEE Standard 1241-2000.

[18] A. V. Oppenheim and R. W. Schafer, "Digital signal processing," United States of America: Alan V. Oppenheim and Bell Laboratories, 1975.

[19] T. W. Parks, and C. S Burrus, "Digital filter design," New York: John Wiley & Sons, 1987.

[20] G. D'Antona and A. Ferrero, "Digital signal processing for measurement systems," United States of America: Springer Science+Business Media, Inc. 2006.

[21] N. Björsell, O. Anderson, and P. Händel,"High dynamic test-bed for characterization of analogue-to-digital converters up to 500MSPS," *10th Workshop on ADC modeling and testing,* Gdynia, Poland, pp. 601-604, 2005.